Cell Research

www.nature.com/cr
www.cell-research.com

LETTER TO THE EDITOR

# m$^6$A promotes R-loop formation to facilitate transcription termination

*Cell Research* (2019) 29:1035–1038; https://doi.org/10.1038/s41422-019-0235-7

Dear Editor,

R-loops are three-stranded nucleic acid structures consisting of a DNA:RNA heteroduplex and a displaced single DNA strand. They constitute a prevalent genomic feature with important functions in all kingdoms of eukaryotes.[1–3] For example, R-loops have been found over unmethylated CpG island promoters, G-rich terminators, and many other regulatory chromosomal loci.[2,3] Moreover, they are essential for diverse cellular processes, such as immunoglobulin class switching, mitotic chromosome segregation,[4] DNA replication and repair, genome stability regulation,[5] as well as in multiple steps during transcription.[6,7] R-loops can be formed both *in cis* and *in trans*; *cis* R-loops are formed between a nascent RNA and its DNA template following transcribing RNA polymerases and exert co-transcriptional regulatory effects.[3,8] Therefore, it is important to control their formation and resolution, and many external factors have already been identified for this process.[7] However, it is still unknown whether the intrinsic properties of the RNA itself, such as various modifications, can modulate the formation of DNA:RNA hybrids.

N6-methyladenosine (m$^6$A) is the most abundant reversible RNA modification, which plays critical roles in various post-transcriptional processes.[9–12] It is installed co-transcriptionally by the methyltransferase complex comprising METTL3, METTL14, WTAP and other factors.[9,13] Yet we have little knowledge of its co-transcriptional functions. Here we investigate the possibility that m$^6$A modification regulates co-transcriptional R-loop formation and/or resolution. First, we confirmed that the m$^6$A level in chromatin-associated RNA (caRNA) was significantly reduced in the absence of the major methyltransferase METTL3 (shMETTL3; Supplementary information, Fig. S1a). Then we applied dot blot assays using anti-R-loop antibody (S9.6) in various cell lines to detect R-loop changes upon METTL3 depletion (Supplementary information, Data S1). We observed a 10-fold decrease in overall R-loop level in shMETTL3 cells compared to that in control HeLa cells, while RNase H treatment substantially eliminated the R-loop signal in both shMETTL3 and control HeLa cells (Fig. 1a and Supplementary information, Fig. S1b). In addition, similar results were obtained in both HeLa and 293F cells via siRNA-mediated METTL3 knockdown (Supplementary information, Fig. S1c–g and Table S1) and were further validated by the reduction in the immunofluorescence signal from nucleoplasmic R-loops (Supplementary information, Fig. S1h). To confirm that this effect is due to m$^6$A methylation, we knocked down additional components of the methyltransferase machinery, i.e., METTL14, WTAP, and KIAA1429. The R-loop level was decreased significantly upon elimination of these components (Supplementary information, Fig. S1c–e). However, depletion of the nuclear m$^6$A reader protein YTHDC1 did not affect the R-loop level (Supplementary information, Fig. S1i, j). Together, these results established a positive correlation between m$^6$A modification and R-loop accumulation. To clarify the physical presence of m$^6$A in R-loops, we performed ultra-high-performance liquid chromatography with multiple reaction monitoring tandem mass spectrometry (UHPLC-MRM-MS/MS) to quantify the m$^6$A composition of RNA in R-loops compared to that in full-length caRNA. Specifically, we treated genomic DNA (gDNA) with RNase III prior to R-loop enrichment to cleave off RNA extensions that form double-stranded RNA (dsRNA) structures outside of R-loops. UHPLC-MRM-MS/MS measurements showed a ~1.5-fold enrichment of m$^6$A modifications in R-loops relative to that in total caRNA (Fig. 1b and Supplementary information, Fig. S1k), suggesting that m$^6$A-modified RNA is present in R-loops.

To define R-loop formation on the genome-wide scale, we employed single-strand DNA ligation-based library construction from DNA:RNA hybrid immunoprecipitation followed by sequencing (ssDRIP-seq;[1] Supplementary information, Fig. S2a) for keeping strand specificity and high reproducibility (Supplementary information, Fig. S2b). We found that R-loops formed by m$^6$A-containing protein-coding transcripts (m$^6$A$^+$ genes) were significantly affected by METTL3 depletion (Fig. 1c). m$^6$A modification sites in caRNA were defined through m$^6$A individual-nucleotide resolution crosslinking and immunoprecipitation linked with high-throughput sequencing (miCLIP-seq) (Supplementary information, Table S2). The miCLIP-seq results demonstrated strong enrichment of m$^6$A modifications near the stop codon in caRNA, and a similar distribution was found in mature mRNA and RiboMinus RNA (total RNA subjected to rRNA depletion) (Supplementary information, Fig. S2c, d). Notably, we observed a significant reduction in R-loop levels around transcription end sites (TESs) of m$^6$A$^+$ genes upon METTL3 knockdown (Fig. 1c). Both promoters and terminators have been found to be major hotspots of R-loop formation.[14] To quantify this regional specificity in R-loop distribution changes, we scanned the genome with nonoverlapping, 200-nt sliding windows and divided these windows into 6 groups: promoters, terminators, and four quarters of the gene bodies. At m$^6$A$^+$ gene loci, the number of R-loops around the TESs was decreased markedly upon METTL3 knockdown, whereas in promoter regions, increases and decreases in the number of R-loops were observed at almost the same frequency (Fig. 1d). Intriguingly, even in the last quarter of the gene body preceding the TES, significantly more loci exhibited a decrease in the number of R-loops than an increase (Fig. 1d). In contrast, for genes whose transcripts do not harbor m$^6$A modification sites (m$^6$A$^-$ genes), there was a much less significant or even nonsignificant difference between the number of genes with increased R-loops and that of those with decreased R-loops in these regions (Fig. 1e and Supplementary information, Fig. S3a), demonstrating a distinct relationship between R-loops and m$^6$A sites.

To further dissect the impact of m$^6$A modification on R-loop formation, we grouped R-loops according to their distance from m$^6$A sites. We found that the closer R-loops are to m$^6$A sites, the greater the reduction in the R-loop level is caused by METTL3 depletion (Fig. 1f). Consistent with this finding, a higher degree of R-loop reduction was observed in m$^6$A$^+$ genes in which m$^6$A modification was strongly affected by METTL3 knockdown than in genes that showed a weaker effect, as well as in m$^6$A$^-$ genes (Fig. 1g), indicating a positive correlation between R-loop

Received: 25 August 2019 Accepted: 5 September 2019
Published online: 12 October 2019

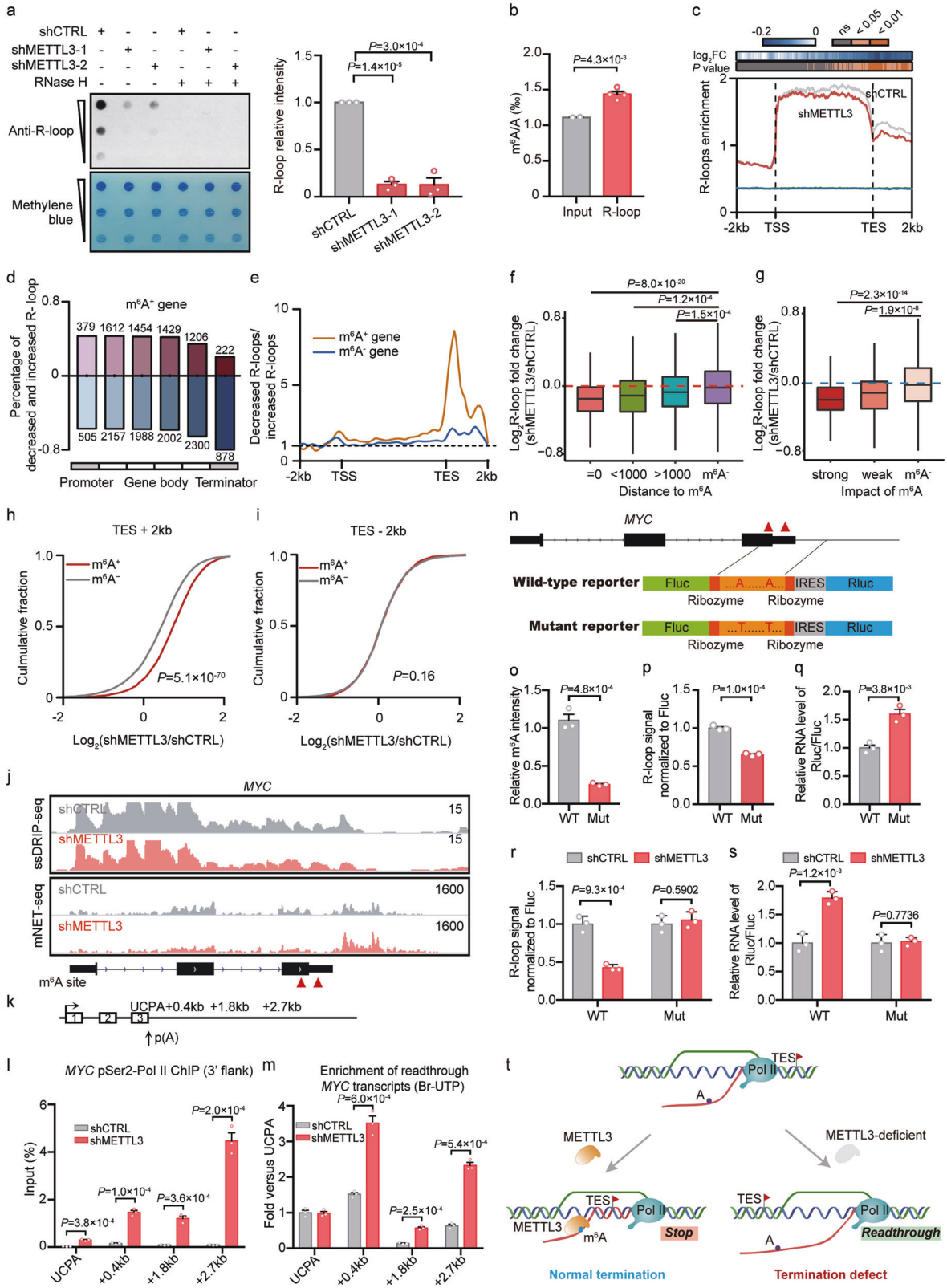


accumulation and m$^6$A modification for not only the direction but also the magnitude of the changes. Genomic visualization of ssDRIP-seq data for *MORF4L2* and *DPF2* genes further confirmed this finding (Fig. S3b). Additionally, the function of METTL3 in promoting R-loop formation is dependent on its m$^6$A methyltransferase activity, as both the dot blot assay and ssDRIP-seq results showed that R-loop reduction upon METTL3 depletion was rescued only by wild-type METTL3, not by the catalytically inactive mutant (Supplementary information, Figs. S2e and S3c–f). These results clearly indicate that METTL3-mediated m$^6$A RNA modification is responsible for R-loop formation in m$^6$A$^+$ genes around TESs.

**Fig. 1** m$^6$A promotes R-loop formation to facilitate transcription termination. **a** Dot blot assay and quantitative analysis of R-loops upon METTL3 knockdown. RNase H treatment was performed as the control treatment. Methylene blue staining indicates equal DNA loading. **b** Quantification of m$^6$A levels demonstrated as bar plots comparing input and DRIPed RNA samples. **c** Metaplot of R-loop enrichments from m$^6$A$^+$ genes in shCTRL (gray) and shMETTL3 (red) cells. R-loop enrichments in randomized regions are shown as the green (shCTRL) and blue (shMETTL3) lines. **d** The number of windows with decreased (blue) and increased (purple) R-loop levels in the promoter region, four quarters of the gene body and the terminator region of m$^6$A$^+$ genes. **e** The ratio of decreased to increased R-loop window numbers in m$^6$A$^+$ genes (orange) and m$^6$A$^-$ genes (blue). **f**, **g** Box plots showing that R-loop fold changes (shMETTL3 vs. shCTRL) in terminator regions are influenced by their distance to m$^6$A (**f**) and the strength of m$^6$A modification (**g**). **h**, **i** Cumulative distributions showing changes of readthrough in regions from TES to 2 kb downstream (**h** TES + 2 kb) and from 2 kb upstream to TES (i TES-2kb) in m$^6$A$^+$ and m$^6$A$^-$ genes. **j** Genomic visualization of ssDRIP-seq and mNET-seq on *MYC* gene. m$^6$A modification sites are shown by red triangles. **k** Structure of *MYC* gene. **l** pSer2-Pol II ChIP with probes downstream of TES of *MYC*. **m** Br-UTP NRO analysis of *MYC*. **n** Cartoon for the minigene reporter system. The *MYC* gene terminator region, which contains m$^6$A sites (red triangles) or mutated sites, was inserted into a dual luciferase reporter vector. **o**–**q** Quantification of m$^6$A (**o**), R-loops (**p**) and readthrough products (**q**) shown as bar plots comparing wild-type and mutant reporters. **r**, **s** Quantification of R-loops (**r**) and readthrough products (**s**) of the wild-type and mutant reporters upon METTL3 depletion. **t** Working model showing that METTL3 installs m$^6$A methylation to nascent RNAs and promotes R-loop formation in the terminator regions to facilitate transcription termination. The error bars of **a**, **l**, **m**, and **o**–**s** indicate ± SEM ($n = 3$). *P* values of **a**–**c**, **l**, **m**, and **o**–**s** were calculated using Student's *t*-test. *P* values of **f**–**i** determined by Mann–Whitney *U* test are shown

R-loop-mediated RNA Polymerase stalling has been reported as a critical factor in transcription termination.[8] Based on our findings that METTL3 stabilizes R-loops around TESs, we hypothesized that METTL3 plays critical roles in regulating transcription termination through m$^6$A modification of caRNA in R-loops. Mammalian native elongating transcript sequencing (mNET-seq) signal downstream of the termination site indicates readthrough activity of elongating Pol II (with CTD phosphorylated at Ser2, pSer2-Pol II) beyond TES due to termination defects. We observed that m$^6$A$^+$ genes showed a significant increase of readthrough levels after TES than m$^6$A$^-$ genes upon METTL3 depletion (Fig. 1h and Supplementary information, Fig. S4a, b). Such difference of mNET-seq signal was not observed upstream of TES between m$^6$A$^+$ and m$^6$A$^-$ genes (Fig. 1i). These results support a specific role of METTL3 in the regulation of transcription termination. Furthermore, we confirmed the effect of knocking down METTL3 on the transcriptional termination of the model genes *MYC* and *ACTB*, which also harbor m$^6$A modification sites around the TESs (Fig. 1j and Supplementary information, Fig. S4c). Consistent with the R-loop levels in other m$^6$A$^+$ genes, the R-loop levels around the TESs of these genes were reduced in METTL3-depleted cells (Fig. 1j and Supplementary information, Fig. S4c). We next performed ChIP-qPCR to confirm the enrichment of pSer2-Pol II beyond TES (Fig. 1k, l and Supplementary information, Fig. S4d, e) and found that pSer2-Pol II chromatin retention was increased over termination regions and even extended 2.7 kb downstream of the TES in *MYC* in shMETTL3 cells (Fig. 1k, l). Br-UTP nuclear run-on (NRO) analysis, which labels only nascent RNA from actively transcribing Pol II, detected a significant enrichment of nascent readthrough transcripts over the termination region in shMETTL3 cells as well (Fig. 1m and Supplementary information, Fig. S4f). This finding was consistent with the function of R-loops in stalling actively transcribing Pol II at TESs to prevent readthrough.[8] Furthermore, the enhanced readthrough of Pol II upon METTL3 knockdown was suppressed by wild-type METTL3 but not its catalytically inactive mutant (Supplementary information, Fig. S4g–i). These results suggest that METTL3-mediated m$^6$A promotes R-loop formation to facilitate transcription termination.

To further investigate the effect of m$^6$A on R-loops and transcription termination, we constructed a minigene reporter system (Fig. 1n). This system allows the transcription of Firefly luciferase (Fluc) and Renilla luciferase (Rluc) reporter genes from a single promoter upstream of Fluc. The two reporters are separated with an R-loop forming region containing two wild-type m$^6$A modification sites cloned from the endogenous *MYC* terminator region (WT). R-loop formation and efficient termination will produce only Fluc transcripts, while reductions in R-loop formation and consequent termination defects will generate readthrough transcripts. Readthrough transcripts carrying the self-cleaving ribozyme will be processed and translated into both Fluc and Rluc reporters from the same transcript. The meRIP-qPCR results showed that A to U mutations of the m$^6$A modification sites diminished m$^6$A modification (Fig. 1o). Furthermore, our results showed that these mutations caused a reduction in R-loop accumulation of ~40% (Fig. 1p), accompanied by an increase of ~1.5-fold in readthrough products (Fig. 1q), indicating a direct effect of m$^6$A on R-loops and consequently on transcription termination. In addition, knocking down METTL3 reduced the m$^6$A level in the WT reporter but not the mutant one (Supplementary information, Fig. S4j), and consequently only reduced R-loop (Fig. 1r) and increased readthrough (Fig. 1s) in the former system.

In summary, our work revealed the crucial role of modulating an intrinsic property of RNA, m$^6$A modification, in promoting co-transcriptional R-loops to prevent readthrough activity of Pol II for efficient termination. Depletion of the m$^6$A methyltransferase METTL3 dramatically reduces R-loop accumulation in m$^6$A$^+$ genes around TESs and perturbs termination. Restoration of R-loops at affected TESs and suppression of consequent readthrough activities require the methyltransferase activity of METTL3 (Fig. 1t). Such regulatory effects of METTL3 on R-loop and Pol II suggest the existence of additional adapter proteins bridging METTL3-Pol II interaction. Further investigation of proteins that can mediate these interactions shall shed light on the underlying mechanisms.

## ACKNOWLEDGEMENTS

This work was supported by grants from the state Key Program of National Natural Science Foundation of China (31430022), the Strategic Priority Research Program of the Chinese Academy of Sciences, China (XDA16010500), CAS Key Research Projects of the Frontier Science (QYZDY-SSW-SMC027), and the NSFC consulting grant (91753000), the National Natural Science Foundation of China (31625016, 31970597). The Sun Lab was supported by Tsinghua University Initiative Scientific Research Program, Tsinghua-Peking Joint Center for Life Sciences, and the 1000 Young Talent Program of China. W.X. was supported by postdoctoral fellowship from Tsinghua-Peking Joint Center for Life Sciences. The Ren Lab was Supported by CAS Pioneer Hundred Talents Program. We thank H.L.W. and C.L at Research Center for Eco-Environmental Sciences, Chinese Academy of Sciences, for their support for UHPLC-MRM-MS/MS analysis.

## AUTHOR CONTRIBUTIONS

Y.G.Y., Q.S. and J.R. conceived the project and supervised all the experiments; X.Y. and Q.L.L. performed most experiments with help from Y.Y., J.C. and L.F.J.; X.Y., W.X., Q.L.L. and Y.Y. performed high-throughput sequencing; Y.C.Z. and W.X. performed bioinformatics analysis with the help of K.L. and Y.S.C.; Y.G.Y, Q.S., J.R., Y.Y., X.Y. and W.X. analyzed the data and wrote the manuscript.

## ADDITIONAL INFORMATION

**Supplementary information** accompanies this paper at https://doi.org/10.1038/s41422-019-0235-7.

**Competing interests:** The authors declare no competing interests.

Xin Yang[1], Qian-Lan Liu[1,2], Wei Xu[3], Yi-Chang Zhang[1,2], Ying Yang[1,2,4], Lin-Fang Ju[1,2], Jing Chen[1,2], Yu-Sheng Chen[1,2], Kuan Li[3], Jie Ren[1,2,4,5], Qianwen Sun[3] and Yun-Gui Yang[1,2,4,5]

*[1]CAS Key Laboratory of Genomic and Precision Medicine, Collaborative Innovation Center of Genetics and Development, School of Future Technology, Beijing Institute of Genomics, Chinese Academy of Sciences, Beijing 100101, China; [2]University of Chinese Academy of Sciences, Beijing 100049, China; [3]Tsinghua-Peking Joint Center for Life Sciences, School of Life Sciences, Tsinghua University, Beijing 100084, China; [4]Institute for Stem Cell and Regeneration, Chinese Academy of Sciences, Beijing 100101, China and [5]Sino-Danish College, University of Chinese Academy of Sciences, Beijing 101408, China*

*These authors contributed equally: Xin Yang, Qian-Lan Liu, Wei Xu, Yi-Chang Zhang*

*Correspondence: Jie Ren (renjie@big.ac.cn) or Qianwen Sun (sunqianwen@mail.tsinghua.edu.cn) or Yun-Gui Yang (ygyang@big.ac.cn)*

## REFERENCES

1. Xu, W. et al. *Nat. Plants* **3**, 704–714 (2017).
2. Chen, L. et al. *Mol. Cell* **68**, 745–757.e5 (2017).
3. Chédin, F. *Trends Genet.* **32**, 828–838 (2016).
4. Kabeche, L. et al. *Science* **359**, 108–113 (2018).
5. Hamperl, S. et al. *Cell* **170**, 774–786 (2017).
6. Sun, Q. W. et al. *Science* **340**, 619–621 (2013).
7. Santos-Pereira, J. M. & Aguilera, A. *Nat. Rev. Genet.* **16**, 583–597 (2015).
8. Proudfoot, N. J. *Science* **352** (2016).
9. Yang, Y. et al. *Cell Res.* **28**, 616–624 (2018).
10. Song, J. & Yi, C. *ACS Chem. Biol.* **12**, 316–325 (2017).
11. Peer, E., Rechavi, G. & Dominissini, D. *Curr. Opin. Chem. Biol.* **41**, 93–98 (2017).
12. Roundtree, I. A. et al. *Cell* **169**, 1187–1200 (2017).
13. Ke, S. D. et al. *Gene Dev.* **31**, 990–1006 (2017).
14. Sanz, L. A. et al. *Mol. Cell* **63**, 167–178 (2016).